Dalton Transactions

RSC Publishing

PAPER

View Article Online
View Journal | View Issue

Cite this: *Dalton Trans.*, 2013, **42**, 16949

A quest for supramolecular gelators: silver(I) complexes with quinoline-urea derivatives†

Dario Braga, Simone d'Agostino,* Eros D'Amen, Fabrizia Grepioni,* Damiano Genovese, Luca Prodi and Massimo Sgarzi

Received 11th July 2013,
Accepted 13th September 2013

DOI: 10.1039/c3dt51873f

www.rsc.org/dalton

The quinoline urea derivatives 1,3-di(quinolin-5-yl)urea (DQ5U), 1-phenyl-3-(quinolin-6-yl)urea (PQ6U), 1-(isoquinolin-5-yl)-3-phenylurea (PiQ5U) and 1-phenyl-3-(3,5-bis(pyrid-2-yl)-1,2,4-triazol-4-yl)urea (PPT4U) have been synthesised and structurally characterized by powder and single crystal X-ray diffraction. Their gelator behaviour in the formation of Ag-complexes has been explored. Compound DQ5U proved capable of gelating the mixed solvent EtOH–DMF 1 : 2 (v/v) when mixed with 1 equivalent of $AgNO_3$. In the case of PQ6U, two polymorphic forms of the complex $[Ag(PQ6U)_2]NO_3$, plus the solvated form $[Ag(PQ6U)_2]NO_3{\cdot}CH_3CN$, were crystallized. Photophysical characterization of the ligands has been conducted in solution, while fluorescence microscopy has been used to examine the microstructure and photophysical properties of the gels formed by PQ5U and DQ5U with $AgNO_3$.

Introduction

Supramolecular gels[1] are a class of soft materials that have gained extensive research interest in recent years. They can be formed when low molecular weight gelators (LMWGs)[2] self-assemble *via* non-covalent interactions such as hydrogen bonds, π-stacking and metal–ligand coordination.[1,2] In materials chemistry, they are good candidates for several applications, such as media for controlling the growth of nanoparticles[3] or crystals of pharmaceuticals,[4] and for drug delivery,[5] amongst others.[6,7] Therefore the quest for new gelators and gelling conditions is an extremely active field of research.[8]

We recently reported[9] that 1-phenyl-3-(quinolin-5-yl)urea (PQ5U),[10] in the presence of the salt $AgNO_3$, behaves as a supergelator of alcohols (such as MeOH, EtOH, *n*-PrOH, i-PrOH and *n*-BuOH) and acetonitrile.[9] This observation prompted us to explore the possibility of "engineering" a class of soft-materials based on the quinolinyl-urea backbone. To this end, we synthesized the following possible candidates to be used as ligands for supramolecular gelation with $AgNO_3$: two isomers of the ligand PQ5U, namely 1-(isoquinolin-5-yl)-3-phenylurea (PiQ5U) and 1-phenyl-3-(quinolin-6-yl)urea (PQ6U), the ligand 1,3-di(quinolin-5-yl)urea (DQ5U); a bis-pyridyl-triazole derivative of urea, *i.e.* 1-(3,5-bis(pyrid-2-yl)-1,2,4-triazol-4-yl)-3-phenylurea (PPT4U), was also synthesized and its behaviour tested (see Scheme 1).

In this paper, we report the full structural characterization of the synthesized molecules, together with an investigation of their ability to form Ag^+-complexes, with the aim to establish

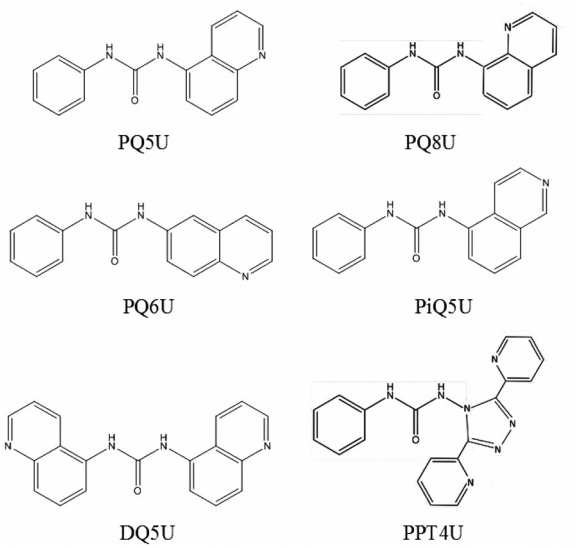

Scheme 1 The ligands 1-phenyl-3-(quinolin-5-yl)urea (PQ5U,[10] previously studied by us[9]), 1-phenyl-3-(quinolin-8-yl)urea (PQ8U[10]), 1-phenyl-3-(quinolin-6-yl)urea (PQ6U), 1-(isoquinolin-5-yl)-3-phenylurea (PiQ5U), 1,3-di(quinolin-5-yl)-urea (DQ5U) and 1-phenyl-3-(3,5-bis(pyrid-2-yl)-1,2,4-triazol-4-yl)urea (PPT4U). PQ6U and PiQ5U are isomers of PQ5U.

Dipartimento di Chimica G. Ciamician, Università di Bologna, Via Selmi 2, 40126 Bologna, Italy. E-mail: fabrizia.grepioni@unibo.it

†Electronic supplementary information (ESI) available: Comparison between experimental and calculated XRPD patterns, Ortep drawings, ^{1}H-NMR spectra, map of fluorescence spectra *vs.* excitation wavelength for the $AgNO_3$:DQ5U gel. CCDC 949683–949690. For ESI and crystallographic data in CIF or other electronic format see DOI: 10.1039/c3dt51873f

whether coordination compounds of these ligands are able to form molecular gels in alcohols and/or in other solvents.

Results and discussion

The ligands: PQ6U, PiQ5U, DQ5U and PPT4U

In this section, a brief description of the molecular and crystal structures of all the ligands discussed in this paper is reported, as determined from single crystal or powder X-ray diffraction (*vide infra*).

The structure of the compound PQ6U was solved and refined from powder data (see the Experimental section for details). The solid-state structure of PQ6U is characterized by the presence of the urea head-to-tail interaction,[11] which is responsible for the formation of the well-known "urea-tape" motif (see Fig. 1a), also detected in crystalline PQ5U and PQ8U (Fig. 1b and c).[10] As shown in Fig. 2, the bifurcated N–H···O interaction [N···O = 2.871(7)–2.907(7) Å] involving two consecutive molecules generates an infinite ribbon-like structure, which extends in the crystal parallel to the *b*-axis.

The same urea-tape motif is also present in both crystalline PiQ5U [N···O = 2.805(4)–2.919(4) Å] (see Fig. 3 and 4) and DQ5U [N···O = 2.858(4) Å]. Weak π-stacking interactions between the quinoline moieties within the ribbons contribute to the stabilization of the crystalline edifice.

Crystalline PPT4U was obtained in two polymorphic modifications, which we call Form I and Form II, differing only slightly in their conformation, as can be seen in Fig. 5.

Fig. 6 shows a comparison of the main packing feature in the two polymorphs. As can be noted, a different tape-like arrangement, with respect to the urea-tape, is present in both solids, formed *via* N–H···N hydrogen bonding interactions between the N–H moieties belonging to the urea group and two nitrogen atoms on an adjacent molecule, one belonging to one pyridyl fragment, the other to the triazole ring [$N(H)\cdots N_{pyr}$ = 2.968(2) Å, $N(H)\cdots N_{triazole}$ = 3.011(2) Å and $N(H)\cdots N_{pyr}$ = 2.992(5) Å, $N(H)\cdots N_{triazole}$ = 3.150(3) Å for Form I and II, respectively].

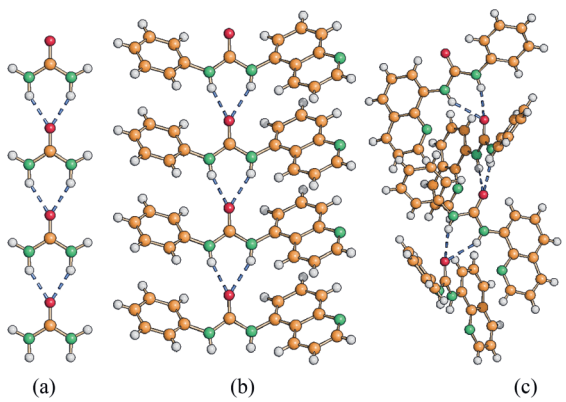

Fig. 1 The hydrogen bonding pattern known as the "urea tape motif" present in crystalline urea (a) and in ligands PQ5U and PQ8U (ref. codes UREAXX09, VUKHUF and VUKJER, respectively).

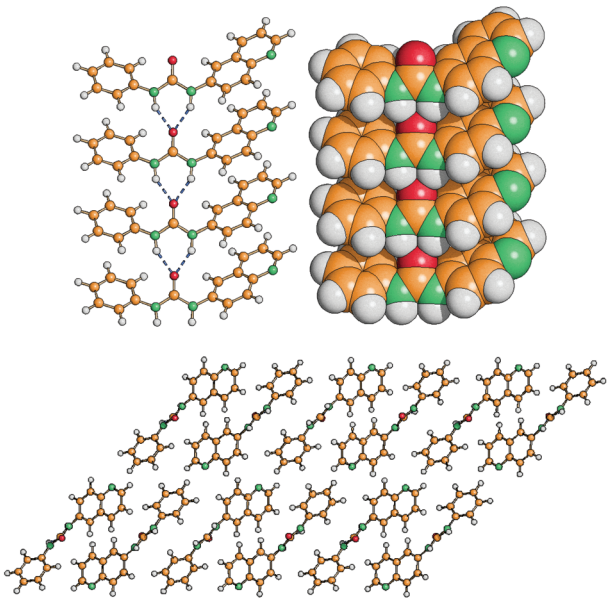

Fig. 2 Top: the urea tape motif extending along the *b*-axis direction in crystalline PQ6U; the van der Waals picture on the right shows the π-stacking interactions along the tape. Bottom: view down the *b*-axis, showing the relative arrangement of the infinite tapes.

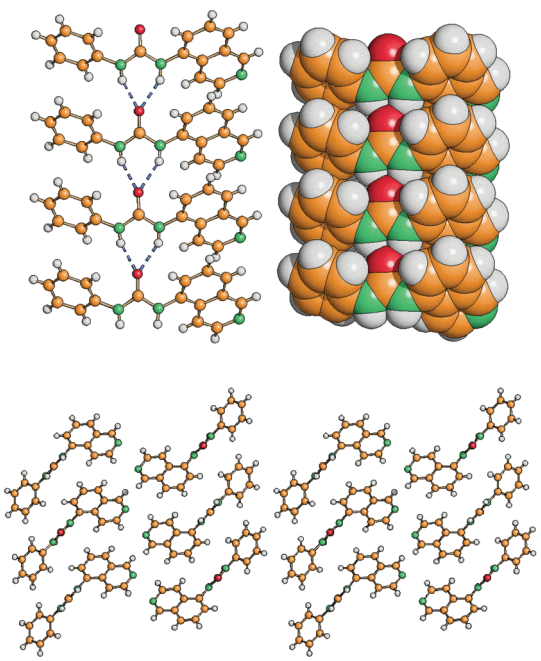

Fig. 3 Top: the urea tape motif extending in the *b*-axis direction in crystalline PiQ5U; the van der Waals picture on the right shows the π-stacking interactions along the tape. Bottom: view down the *b*-axis, showing the relative arrangement of the infinite tapes.

The differences between the two polymorphic modifications are due to the fact that in Form I, adjacent molecules are referred by a screw-axis along the *b*-axis direction in the $P2_1/c$ space group, while in Form II adjacent molecules along the tape are simply related by translation along the *a*-axis direction

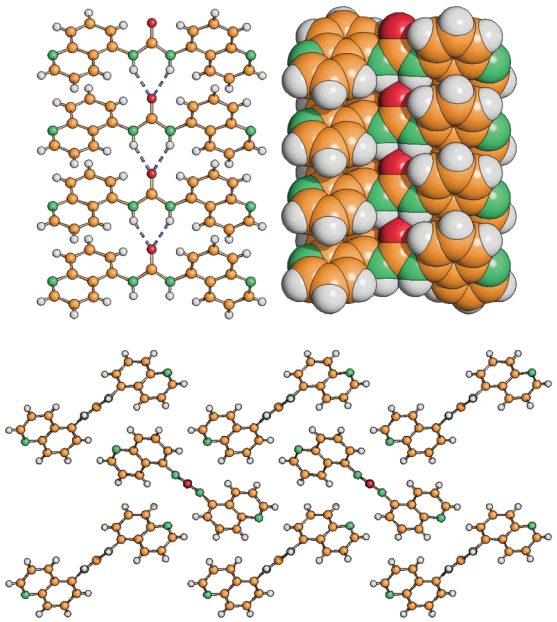

Fig. 4 Top: the urea tape motif extending along the *a*-axis in crystalline DQ5U; the van der Waals picture on the right shows the π-stacking interactions along the tape. Bottom: view down the *a*-axis, showing the relative arrangement of the infinite tapes.

Fig. 5 Superimposition of Form I and Form II molecular structures for crystalline PPT4U, showing that the two conformations are almost exactly the same in the two polymorphs.

in the $P2_1$ space group. Translational repetition in the two cases is evidenced by red arrows in Fig. 6.

Fig. 7 shows how the different arrangements of the hydrogen bonded molecules along the tapes affect the resulting crystal packing in the two forms. In Form I, the presence of C–H···π interactions is also evident, as shown in Fig. 8.

The two polymorphs differ in their morphology also: Fig. 9 shows the rod-like crystals of Form I and the plate-like crystals of Form II, as observed with an optical microscope in polarized light.

Gelation tests and gel characterization

The four compounds 1,3-di(quinolin-5-yl)urea (DQ5U), 1-phenyl-3-(quinolin-6-yl)urea (PQ6U), 1-(3,5-bis(pyrid-2-yl)-1,2,4-triazol-4-yl)-3-phenylurea (PPT4U) and 1-(isoquinolin-5-yl)-3-phenylurea (PiQ5U) were all treated with $AgNO_3$ in order to explore their gelling behavior. When crystals were recovered from the experiments, the crystal structure was also determined (*vide infra*).

In a typical gelation experiment, 10–15 mg of a finely ground ligand–$AgNO_3$ mixture in 1 : 2 (for PiQ5U, PQ6U and

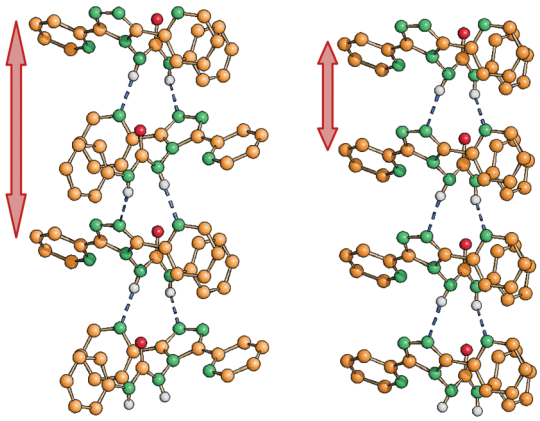

Fig. 6 The tape-like arrangement observed in crystalline Form I (left, tape extending along the *b*-axis direction) and Form II (right, tape extending along the *a*-axis direction). Red arrows evidence the translational repetition in the two forms. H_{CH} omitted for clarity.

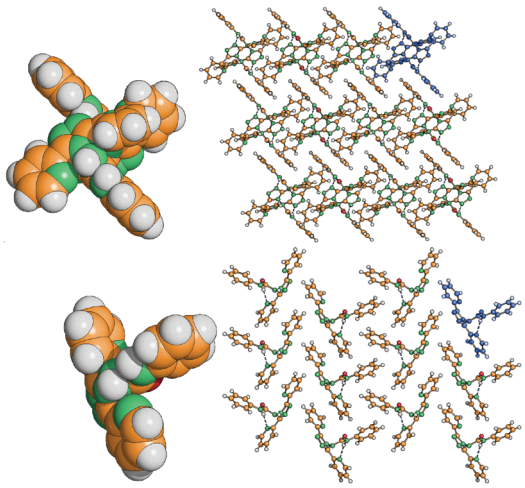

Fig. 7 Projection along the tape direction (left) and overall packing (right, here the tapes shown on the left are coloured blue) in crystalline Form I (top) and Form II (bottom).

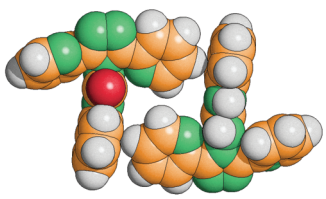

Fig. 8 CH···π interactions in crystalline Form I, involving a pyridyl CH terminus and the phenyl ring on neighbouring molecules belonging to adjacent tapes.

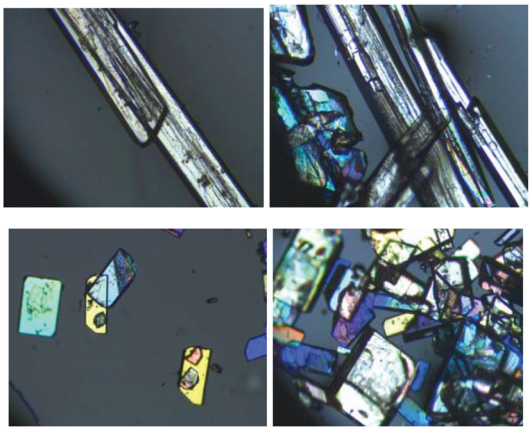

Fig. 9 The different morphology observed for crystals of Form I (top, rods) and Form II (bottom, plates).

PPT4U), or 1 : 1 (for DQ5U) molar ratio was suspended in 5 mL of pure solvent or solvent mixture in a 2 cm diameter vial, and the vial was heated to boiling point, until a clear solution or a fine suspension was obtained, which was allowed to cool to room temperature. The formation of a suspension indicates limited or total insolubility of the ligand even at high temperatures. Table 1 lists the results of the tests.

As can be seen from Table 1, only compound DQ5U was able to act, in association with $AgNO_3$, as a gelator in the presence of the solvent mixture EtOH–DMF 1 : 2 (v/v) when mixed with 1 equivalent of $AgNO_3$. As evidenced by the "tube-inversion" test[1] (see Fig. 10a), the critical gelation concentration[1] (*CGC*, *i.e.* the lowest concentration at which gelation occurs) at room temperature was found to be 0.17% (w/v). Therefore, for this class of compounds, the most highly performing supergelator[1] remains the previously reported complex of $AgNO_3$ with 1-phenyl-3-(quinolin-5-yl)urea (PQ5U).[10]

Once prepared, the gel is stable for one week at room temperature in the presence of air. The dropping-ball method[1] was used to evaluate the gel to sol transition temperature as a function of the gelator concentration (Fig. 10b). Gel formation is

Table 1 Results of the gelling tests with the new ligands and $AgNO_3$ (ligand : $AgNO_3$ molar ratio in parenthesis). I = insoluble ligand, C = single crystals formation, P = precipitate, S = stable solution, G = gel formation

Solvent	PQ6U (2 : 1)	PiQ5U (2 : 1)	DQ5U (1 : 1)	PPT4U (1 : 2)
Water	I	I	I	I
Methanol	C	I	I	S
Ethanol	I	I	I	S
n-Propanol	I	I	I	S
i-Propanol	I	I	I	S
n-Butanol	I	I	I	S
Acetonitrile	C	P	I	S
DMF	S	S	I	S
Toluene	I	I	I	I
Chloroform	I	I	I	I
Butyl-benzoate	I	I	I	I
DMF–EtOH 1 : 2	S	S	I	S
DMF–EtOH 2 : 1	S	S	G	S

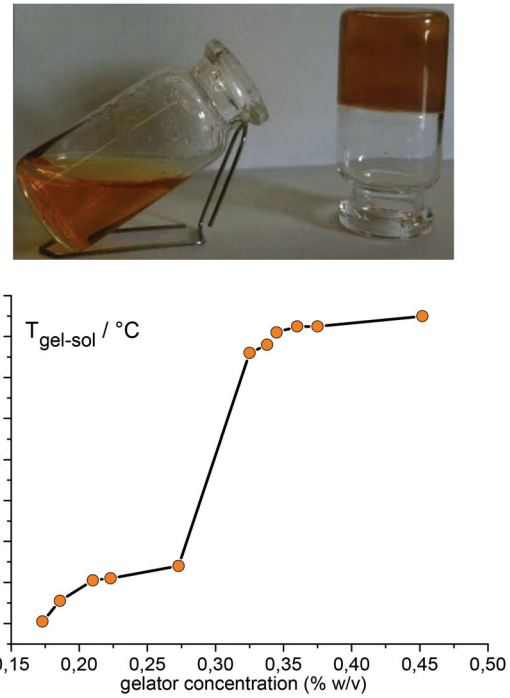

Fig. 10 Top: The $AgNO_3$: DQ5U system in the solvent mixture DMF–EtOH 1 : 2 v/v. A clear sol is obtained at high temperature (left), while the "tube-inversion test" at room temperature shows the presence of a gel (right); bottom: a plot of gel to sol transition temperature *vs.* gelator concentration.

thermoreversible, with gel to sol transition temperatures ranging from 24 °C for 0.17% (w/v) to 37 °C for a 0.325% (w/v); after 3–4 cycles of heating (gel → sol transition) and cooling (sol → gel transition), degradation of the system is observed: a brown solution is obtained at higher temperature that does not gelify upon cooling. The degradation process is presumably due to the reduction of the silver cation.

Photophysical properties

The photophysical characterization of PQ8U, PQ6U, PiQ5U, PQ5U and DQ5U 1×10^{-5} M in ethanol was performed. The absorption spectra of these compounds present an intense band between 242 and 258 nm (ε = 32 500–71 000 M^{-1} cm^{-1}) and a smaller and broader band with a maximum between 307 and 332 nm (ε = 7000–9300 M^{-1} cm^{-1}) (see Table 2). The former can be attributed to a π–π^* transition, while the latter is due to an n–π^* transition.[12] The emission spectra are characterized by a non-structured band with wavelengths at peaks ranging from 386 to 437 nm. These compounds present very different quantum yields, ranging from 6.5×10^{-4} for PQ8U to 1.08×10^{-1} for PQ5U, as shown in Table 2.

A systematic study of these ligands was then performed in order to explore their affinity and photochemical behaviour in the presence of Mg^{2+}, Cu^{2+}, Ag^{+}, Cd^{2+}, Hg^{2+} and NO_3^-, F^-, Cl^-, Br^-, $H_2PO_4^-$, CH_3COO^-. It was checked that triflate and perchlorate anions are not complexed by the ureic moiety of these compounds, and similarly, the tetrabutylammonium cation is not complexed by quinolinic nitrogen: we thus chose them as

Table 2 Photophysical properties of PQ8U, PQ6U, PiQ5U, PQ5U and DQ5U and their complexes in EtOH

Compound	Logarithm of association constant, log K_a	Absorption λ_{max}/nm (ε/M^1 cm^{-1})	Fluorescence λ_{max}/nm	Φ	τ/ns
PQ8U	—	249 (58 000); 331 (8900)	424	6.5×10^{-4}	<0.1
PQ8U·Cu^{2+}	ML 5.53 ± 0.08	270 (42 000); 397 (4000)	422	3.2×10^{-4}	<0.1
PQ8U·F^-	ML <2		428	9.6×10^{-4}	<0.1
PQ6U	—	258 (71 000); 332 (6900)	386	2.9×10^{-2}	0.5
PQ6U·Hg^{2+}	ML 4.74 ± 0.05	370 (7300)	386	2.6×10^{-3}	<0.1
PQ6U·Cu^{2+}	ML 3.96 ± 0.02	375 (4400)	386	8.7×10^{-3}	<0.1
PQ6U·Ag^+	ML 2.66 ± 0.02	260 (76 000); 340 (7500)	386	1.6×10^{-2}	<0.1
PiQ5U	—	246 (32 500); 307 (9300)	396	9.1×10^{-2}	1.2
PiQ5U·Hg^{2+}	ML 4.55 ± 0.02	326 (5900); 355 (4700)	396	1.0×10^{-2}	<0.1
PiQ5U·Cu^{2+}	ML 3.47 ± 0.02	350 (7300)	396	2.3×10^{-2}	<0.1
PQ5U	—	245 (46 500); 316 (7000)	437	1.08×10^{-1}	2.5
PQ5U·Hg^{2+}	ML 4.34 ± 0.04	317 (3100); 380 (5100)	437	7.6×10^{-3}	<0.1
PQ5U·Cu^{2+}	ML 3.69 ± 0.04	350 (5900)	437	5.4×10^{-2}	<0.1
DQ5U	—	242 (46 000); 317 (8700)	434	6.8×10^{-2}	1.3
DQ5U·Hg^{2+}	ML 4.47 ± 0.01	317 (7200); 380 (4400)	434	4.8×10^{-3}	<0.1
DQ5U·Cu^{2+}	ML 3.53 ± 0.02	350 (9200)	434	3.6×10^{-2}	<0.1

counterions for the cationic species listed above. As regards the metal ions, all the compounds can complex Cu^{2+} and Hg^{2+} apart from PQ8U, which does not show affinity toward Hg^{2+}. PQ6U is the only one able to complex also Ag^+ in ethanolic solution (see Table 2) with a $K_a \approx 10^3$ M^{-1}. In all of the cases, the addition of increasing amounts of these metal ions caused changes in the absorption spectra, in particular the decrease of the n–π* band and the appearance of a new bathochromically shifted band centred between 340 and 397 nm (see, for example, the absorption spectrum of PQ6U with Hg^{2+}, Fig. 11a). It is worth noting that this new absorption band allows for selective excitation of the complexed species in a fluorescence imaging setup, as discussed in the next section. The complexation of Cu^{2+}, Hg^{2+}, Ag^+ caused the quenching of the luminescence in the emission spectra (Fig. 11b). The values of log K_a toward Hg^{2+} are similar for all the ligands ($4.34 < \log K_a < 4.74$), and an analogous behavior was found for Cu^{2+} ($3.47 < \log K_a < 3.96$), except for PQ8U exhibiting a higher value (Table 2). No changes either in the absorption or in emission spectra were observed for the addition of NO_3^-, F^-, Cl^-, Br^-, $H_2PO_4^-$, CH_3COO^-, except for PQ8U, which exhibits a low association constant (<10^2) toward F^- with a slight enhancement in the emission spectrum.

Finally, we observed that the presence of water caused a quenching of the luminescence for all the compounds, probably due to the formation of hydrogen bonds stronger than those formed by ethanol molecules.

Photophysics and fluorescence imaging of DQ5U and PQ5U gels

Fluorescence microscopy was used to examine the microstructure of the gels. The fluorescence of the ligands can indeed be used to visualize the fibril aggregates responsible for the gelation process. Fig. 12a–c show the fluorescence of samples at increasing concentration of ligands PQ5U and $AgNO_3$ in ethanol; Fig. 12d–f are fluorescence images of DQ5U and $AgNO_3$ in the ethanol : DMF ratio 1 : 2 at increasing concentration. Since all images were taken with the same RGB camera and the same set of filters, the difference in color corresponds to the different spectral properties of these fluorescent gels, as also proved by the fluorescence spectra shown in Fig. 13.

In Fig. 12b and c the cyan-emitting fine texture is clearly recognizable, which at the highest concentration is extremely homogeneous along the whole sample (millimeter-to-centimeter scale) (Fig. 12c). Such a texture is not present at the lowest concentration at which no gelification is observed (Fig. 12a, only traces of random adhesion on the glass surface are visible). The texture is in some cases strongly oriented, probably due to the local mechanical shear-stress experienced by the gel during sample preparation.

Fig. 12e and f show the presence of large fibrils which are responsible for the gelation of DQ5U in the presence of $AgNO_3$. Differently from what is observed for PQ5U, the length of the fibrils for this ligand is several hundred microns, the width is within few microns and fibrillar interspace is larger than in PQ5U gels. This microstructure strongly determines the macroscopic properties of the gels. At the microscopic scale we indeed observed an increased mobility of the liquid phase within the large spaces visible among the fibrils, and in some cases even the fibrils easily moved across each other, following a general reorganization. DQ5U forms, as a result, much weaker gels than PQ5U at all concentrations, as proved by the gel breaking upon little mechanical stresses.

The photophysical properties of the two gels were explored with fluorescence spectroscopy. When DQ5U makes gel in the presence of Ag^+, it shows a broadened, red-shifted emission band, which is responsible for the green color observed in the fluorescence images. Such green emission can be selectively excited, and thus observed separately from the blue native ligand emission by using excitation wavelength >370 nm (as in our microscope setup) or <300 nm. This observation is consistent with the changes in the DQ5U absorption spectrum, which, upon complexation with metals in diluted solutions,

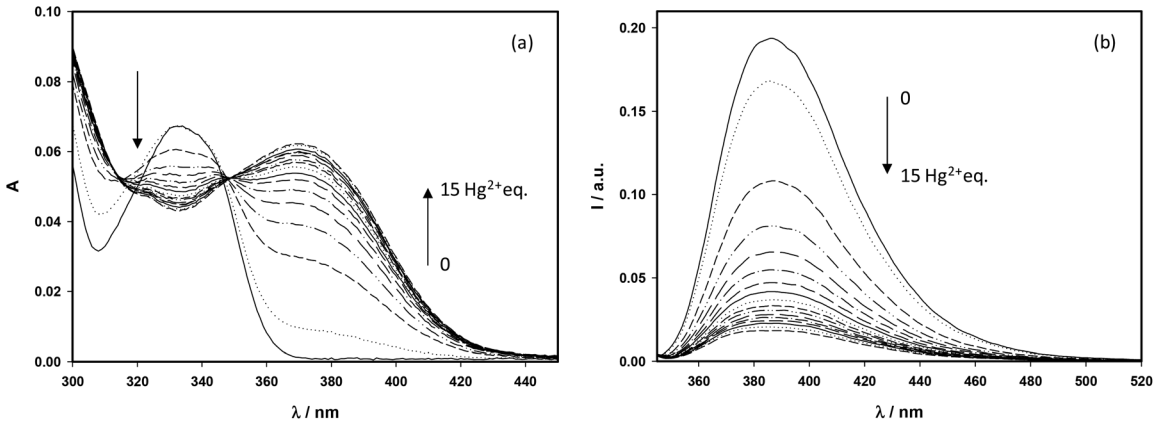

Fig. 11 Absorption (a) and emission (b) spectra of PQ6U (1×10^{-5} M) in EtOH at room temperature upon addition of increasing amounts of Hg^{2+} ions (from 0 to 15 equivalents).

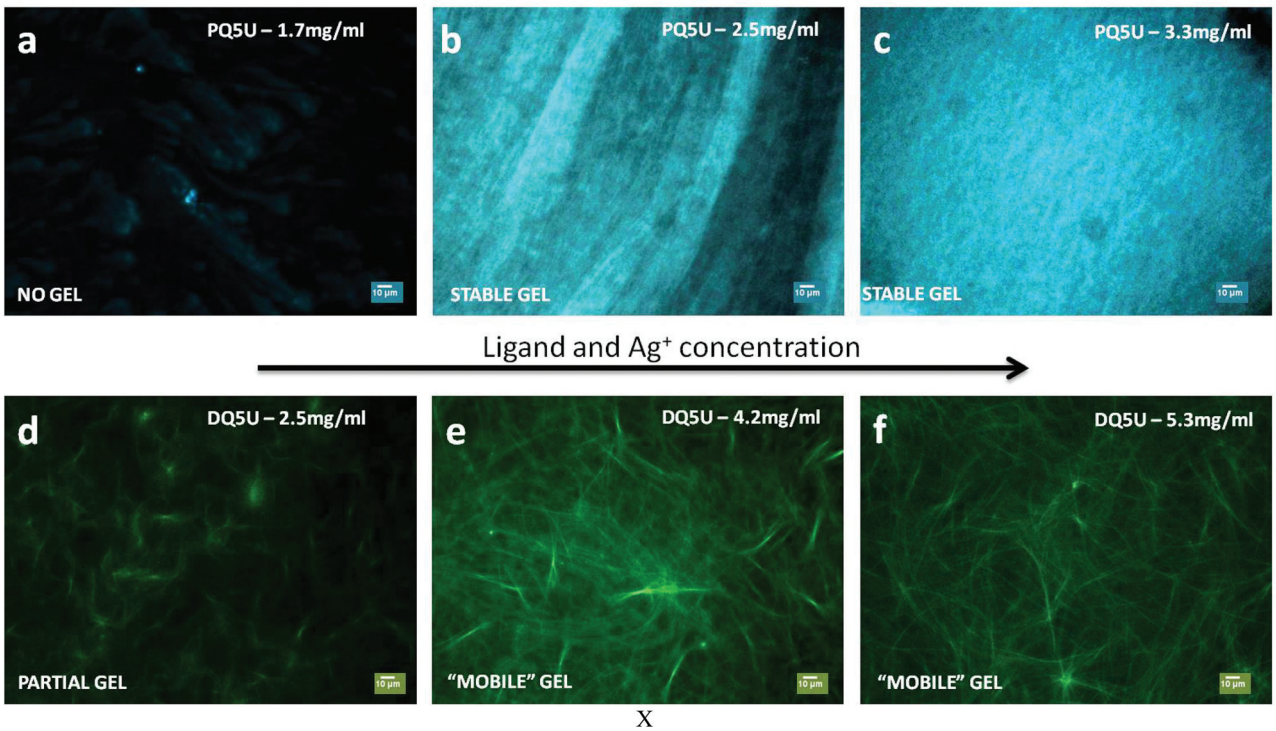

Fig. 12 Fluorescence microscopy images of PQ5U (a–c) and DQ5U (d–f) equimolar with Ag^+ at various concentrations. Note the presence of fibrillar aggregates.

exhibits a decrease in the n–π* band gap and the appearance of a new red-shifted band centred at 380 nm (see Fig. 11a). In contrast, the gels formed by PQ5U do not show any significant shift in the emission band compared to the native ligand. The lifetimes measured for gel emissions were comparable to that observed in dilute solutions: 1.3 ns for DQ5U and 1.4 ns for PQ5U.

Interestingly, the gel emissions show a rather high fluorescence anisotropy ($r \sim 0.3$ for the DQ5U gel and $r \sim 0.2$ for the PQ5U gel), indicating that the emitters do not have much rotational freedom when packed in the fibrillar structure, and that in the case of migration of excitation energy the polarization is maintained, possibly due to the high ligand orientation in the fibrils.

Ag-complexes obtained with the ligand PQ6U: a solvate and two polymorphs of the unsolvated form

When gelation tests were performed in the presence of the ligand PQ6U, three different crystalline materials were recovered from the solutions, which were characterized *via* X-ray single diffraction as an acetonitrile solvate, $[Ag(PQ6U)_2]$-$NO_3 \cdot CH_3CN$, and (in the case of EtOH or MeOH solutions) two polymorphic modifications of the unsolvated complex, $[Ag(PQ6U)_2]NO_3$. No crystalline material suitable for diffraction

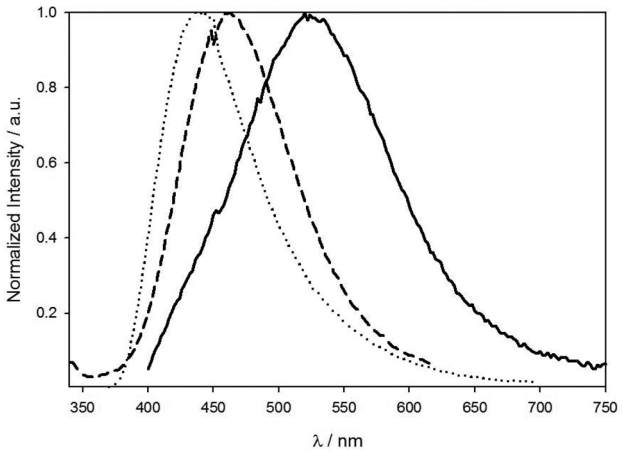

Fig. 13 Fluorescence spectra of DQ5U/Ag^+ gel and PQ5U/Ag^+ gel at different excitation wavelength. Solid line: DQ5U/Ag^+ gel excited at 380 nm. Dotted line: DQ5U/Ag^+ gel excited at 350 nm. Dashed line: PQ5U/Ag^+ gel excited at 330 nm (this emission spectrum is invariant with excitation wavelength). Note that the two emissions of DQ5U/Ag^+ gel attributable to the free ligand and to the fibrils can be separated by selecting the suitable excitation wavelength (350 and 380 nm respectively, see also the emission map in Fig. ESI-9†).

experiments were obtained when DQ5U and PiQ5U were treated with $AgNO_3$.

The solvate $[Ag(PQ6U)_2]NO_3{\cdot}CH_3CN$. The acetonitrile solvate $[Ag(PQ6U)_2]NO_3{\cdot}CH_3CN$ is characterized by the presence of two complex molecules in the asymmetric unit, which differ for the relative conformation of the urea groups with respect to the quinoline-Ag-quinoline fragment (see Fig. 14). The two complexes can therefore be considered conformational isomers: the effect on the Ag^+ coordination geometry is profound, and two distinct patterns can be easily recognized in the crystal. In the first complex isomer the Ag^+ ion is linearly coordinated by two nitrogen atoms from the quinoline units [$Ag^+\cdots N$ = 2.197(5) Å; N–Ag^+–N angle = 180.0(2)°, see Fig. 15a], but two oxygen atoms belonging to two adjacent ligands also interact with the silver cation, [O···N = 2.941(7)–2.981(7) Å] (see Fig. 15a). This results in the formation of a 1-D ribbon, with each PQ6U ligand bridging two silver cations and the urea fragments interacting *via* hydrogen bonds with the nitrate anions on both sides of the ribbon (see Fig. 15b). Two such ribbons

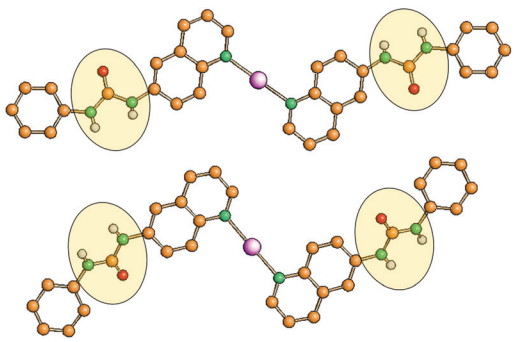

Fig. 14 The two conformational isomers present in the asymmetric unit of $[Ag(PQ6U)_2]NO_3{\cdot}CH_3CN$. H_{CH} atoms omitted for clarity.

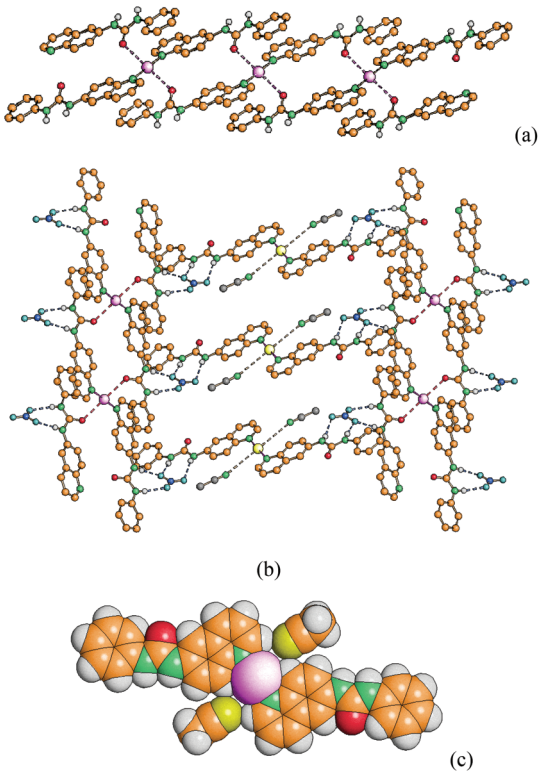

Fig. 15 The 1-D ribbon (a) involving one of the two conformational isomer complexes in crystalline $[Ag(PQ6U)_2]NO_3{\cdot}CH_3CN$, with each PQ6U ligand bridging two silver cations; the urea fragments interact *via* hydrogen bonds with the nitrate anions on both sides of the ribbon (b). The second conformational isomer bridges two such ribbons, *via* HB interactions with the nitrate anions. Solvent molecules (c) interact *via* the N atom with the quinoline moieties. H_{CH} atoms omitted for clarity.

are in turn connected, *via* hydrogen bonds involving the same nitrate groups, with the second conformational isomer (central part of Fig. 15b). The solvent molecules direct the N-extremity towards the silver cation, and interact *via* N···HC interactions with the quinoline moieties, as can be seen in Fig. 15c.

Thermal gravimetric analysis on a polycrystalline sample of $[Ag(PQ6U)_2]NO_3{\cdot}CH_3CN$ shows a weight loss of *ca.* 5% in the temperature range 100–175 °C, corresponding to the loss of one mole of acetonitrile per mole of complex (see ESI†).

Form I of the unsolvated complex $[Ag(PQ6U)_2]NO_3$. Unlike the previously described acetonitrile solvated complex, in crystalline $[Ag(PQ6U)_2]NO_3$, Form I, the coordination geometry of the Ag^+ ion is distorted trigonal, with two quinoline units forming a bent backbone [$Ag^+\cdots N$ = 2.146(3)–2.151(3) Å] and the nitrate anion entering the first coordination sphere (see Fig. 16a) [$Ag^+\cdots O$ = 2.743(3)–2.821(3) Å]. The urea groups on the ligands interact *via* hydrogen bonding with two NO_3^- anions [O···N = 2.922(5)–2.929(4) Å]. The complexes are organized in the solid in a criss-cross pattern (Fig. 16b), with the nitrate anions acting as a "glue" *via* hydrogen bonding interactions, as can be seen in Fig. 16c, which shows how a single anion simultaneously interacts with three cationic complexes.

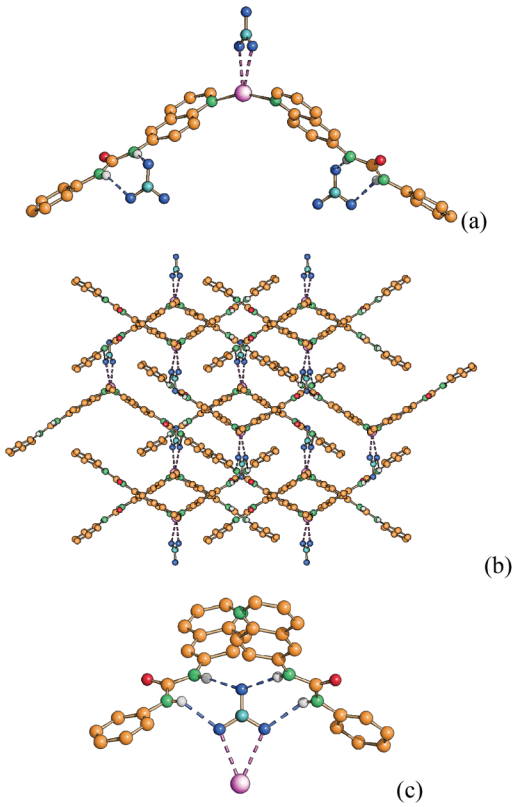

Fig. 16 (a) Coordination sphere around the Ag^+ ion in crystalline $[Ag(PQ6U)_2]NO_3$ Form I, and (b) the criss-cross arrangement of the complexes; the nitrate anions act as a hydrogen bonding "glue" by simultaneously interacting with three neighbouring cationic complexes. H_{CH} atoms omitted for clarity.

A variable temperature X-ray diffraction measurement on a crystalline powder sample of $[Ag(PQ6U)_2]NO_3{\cdot}CH_3CN$ shows that, upon heating the sample to 155 °C, a desolvation process takes place, yielding $[Ag(PQ6U)_2]NO_3$ Form I (Fig. 17).

Form II of the unsolvated complex $[Ag(PQ6U)_2]NO_3$. In crystalline $[Ag(PQ6U)_2]NO_3$, Form II, the two quinoline ligands coordinating the silver cation are oriented so as to form a "tweezer" that traps the nitrate anion, as can be seen from Fig. 18. The neutral unit is then repeated in a head-to-tail fashion, thus forming rows (Fig. 19a) and layers, which are then covered by a second layer shifted so as to fill the cavities below (Fig. 19b).

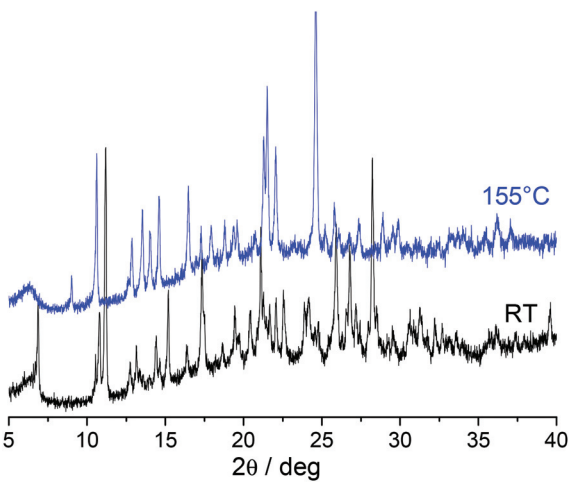

Fig. 17 Variable temperature powder diffraction experiment showing the conversion $[Ag(PQ6U)_2]NO_3{\cdot}CH_3CN \rightarrow [Ag(PQ6U)_2]NO_3$ upon heating.

A fifth polymorphic modification of $[Ag(PQ5U)_2](NO_3)$. In the course of our gelling tests a fifth polymorph of the supramolecular complex $[Ag(PQ5U)_2](NO_3)$, for which four polymorphs had been characterized by us in a previous work,[9] was crystallized from MeOH. For the sake of completion we report here its structure, although the data quality for this complex are not at the level of those reported for polymorphs I–IV.[9]

Fig. 20 shows a comparison of all polymorphic modifications for crystalline $[Ag(PQ5U)_2](NO_3)$: it can be seen that the conformation of the supramolecular complex in Form V closely resembles that of Form IV. Two independent molecules are present in the asymmetric unit; they are connected *via* hydrogen bonds between the urea groups $[N(H)_{urea}\cdots O_{CO}$ = 2.891(2)–2.941(2) Å), thus forming a large supramolecular ring,

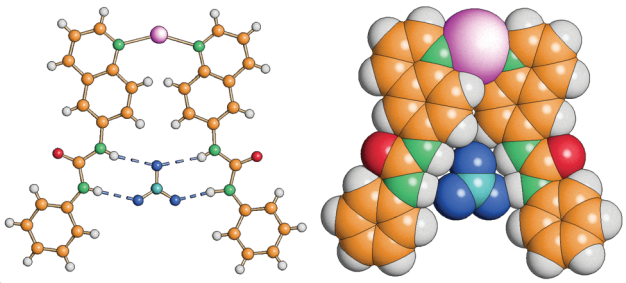

Fig. 18 The "tweezer-like" complex trapping the nitrate anion in crystalline $[Ag(PQ6U)_2]NO_3$ Form II.

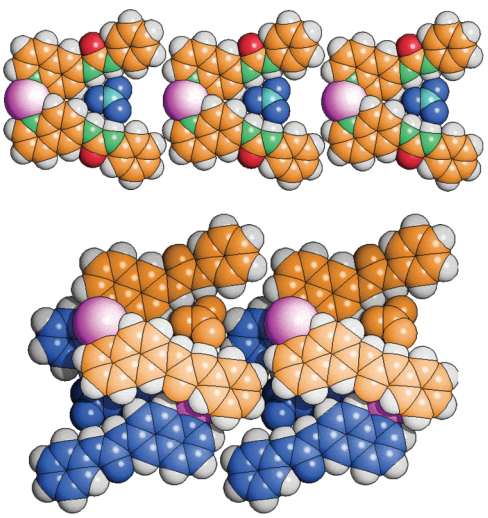

Fig. 19 Rows (top) and layers (bottom) of tweezers in crystalline $[Ag(PQ6U)_2]NO_3$ Form II. A second layer (evidenced in light-orange) filling the underlying cavities is partly shown on top of the first layer.

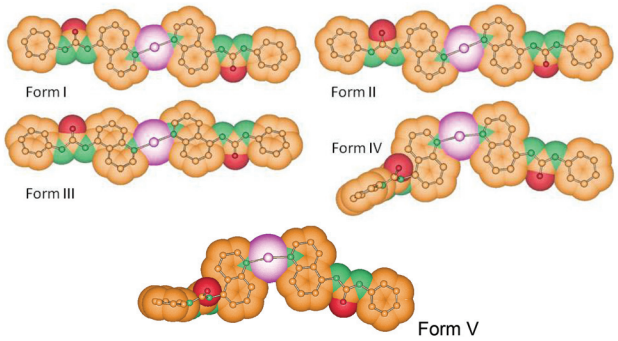

Fig. 20 Comparison of the $[Ag(PQ5U)_2]^+$ units observed in Forms I to IV[9] (copyright RSC) and in Form V. H atoms omitted for clarity.

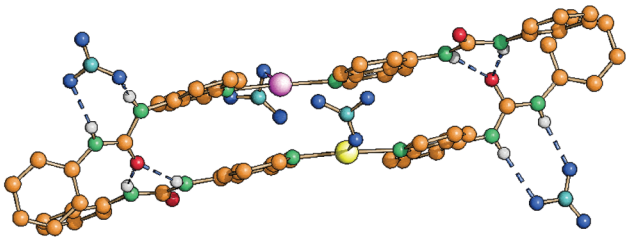

Fig. 21 The supramolecular ring formed by the two independent complexes in crystalline $[Ag(PQ5U)_2](NO_3)$ Form V. H_{CH} omitted for clarity.

to which two nitrate anions are hydrogen bonded [O···N = 2.891(2)–3.171(3) Å], see Fig. 21.

Conclusions

Starting from our findings on the behaviour of compound 1-phenyl-3-(quinolin-5-yl)urea (PQ5U)[9] in the presence of $AgNO_3$ as a supergelator of the alcohols MeOH, EtOH, *n*-PrOH, i-PrOH and *n*-BuOH as well as of acetonitrile[10] we have explored a whole class of new, strictly related, compounds. We have synthesised and structurally characterized by single crystal and powder diffraction the derivatives 1,3-di(quinolin-5-yl)urea (DQ5U), 1-phenyl-3-(quinolin-6-yl)urea (PQ6U), 1-(3,5-bis(pyrid-2-yl)-1,2,4-triazol-4-yl)-3-phenylurea (PPT4U) and 1-(isoquinolin-5-yl)-3-phenylurea (PiQ5U) and examined their gelling behaviors when treated under the same conditions as their parent 1-phenyl-3-(quinolin-5-yl)urea (PQ5U) in the formation of Ag-complexes. Of all compounds, only DQ5U proved capable of gelating a mixture of solvents EtOH–DMF 1 : 2 (v/v) when mixed with 1 equivalent of $AgNO_3$. As evidenced by the "tube-inversion" test, the critical gelation concentration[1] (CGC, *i.e.* the lowest concentration at which gelation occurs) at room temperature was found to be 0.17% (w/v) for the gel DQ5U-$AgNO_3$. Compounds PQ5U and PiQ5U, though strictly related, do not show any gelling behaviour. On the other hand molecule PQ6U forms the stable complexes $[Ag(PQ6U)_2]NO_3{\cdot}CH_3CN$, and $[Ag(PQ6U)_2]NO_3$ when reacted with $AgNO_3$, depending on the solvent. Compound PiQ5U : $AgNO_3$, in contrast, does not yield single crystals or polycrystalline powders suitable for powder diffraction studies.

This study confirms that structure–property relationships are difficult to predict when dealing with gel formation. Even compounds with close structural relationships show very different gelling behaviors or no formation of gels at all. Clearly, prediction of gelling behaviour from a knowledge of the molecular structure of the complexes and of the nature of the solvents is still a chimaera, and the investigator can only tackle the problem by trial-and-error.

Experimental

Synthesis

All reactants and reagents were purchased from Sigma-Aldrich and used without further purification. Reagent grade solvents were used.

Synthesis of 1-phenyl-3-(quinolin-5-yl)urea (PQ5U) and 1-phenyl-3-(quinolin-8-yl)urea (PQ8U). The ligands PQ5U and PQ8U were synthesized according to the literature procedure.[10] 5-Aminoquinoline or 8-aminoquinoline (0.36 g, 2.5 mmol) was dissolved in dry dichloromethane (*ca.* 10 mL); a solution of phenylisocyanate (0.27 mL, 2.5 mmol) in dichloromethane was then added dropwise, and the mixture was stirred at room temperature for 3 h. The products formed were filtered and recrystallized from methanol. PQ5U and PQ8U were identified by X-ray powder diffraction. See Fig. ESI-0.†

Synthesis of 1-phenyl-3-(quinolin-6-yl)urea (PQ6U). 6-Aminoquinoline (72.3 mg, 5 mmol) was dissolved in 15 mL of dry dichloromethane, then a solution of phenylisocyanate (0.54 mL, 5 mmol) in dichloromethane was added dropwise over two hours; the resulting mixture was stirred at RT for an additional two hours. The product formed (white powder) was recovered by filtration and washed with cold dichloromethane (5 × 2 mL). Recrystallization from alcohol (methanol or ethanol) or acetonitrile afforded only a polycrystalline powder. Yield: 85%.

^{1}H-NMR (DMSO-d_6, 400 MHz, ppm): 9.05 (1H, s), 8.8 (1H, s), 8.7 (1H, m), 8.2 (1H, d, J = 8.4 Hz), 8.1 (1H, d, J = 2.4 Hz), 7.9 (1H, d, J = 9.2 Hz), 7.7 (1H, m), 7.4 (3H, m), 7.3 (2H, t, J = 7.2 Hz), 7.0 (1H, t, J = 7.2 Hz). See Fig. ESI-1.†

Synthesis of 1-(isoquinolin-5-yl)-3-phenylurea (PiQ5U). 5-Aminoisoquinoline (72.1 mg, 5 mmol) was dissolved in 15 mL of dry acetone, then a solution of phenylisocyanate (0.54 mL, 5 mmol) in acetone was added dropwise over two hours; the resulting mixture was stirred at RT for an additional four hours. The product formed (brownish powder) was recovered by filtration and washed with cold acetone (5 × 2 mL). Colourless, needle-shaped crystals suitable for X-ray diffraction were obtained by vapor diffusion of water into a dimethylsulfoxide solution of the freshly synthesized ligand. Yield: 75%.

^{1}H-NMR (DMSO-d_6, 400 MHz, ppm): 9.3 (1H, s), 9.0 (1H, s), 8.8 (1H, s), 8.5 (1H, d, J = 6 Hz), 8.2 (1H, d, J = 7.6 Hz), 7.9 (1H, d, J = 6.4 Hz), 7.8 (1H, d, J = 8.4 Hz), 7.6 (1H, t, J = 6.4 Hz), 7.5 (2H, m), 7.3 (2H, m), 7.0 (1H, t, J = 7.6 Hz). See Fig. ESI-2.†

Synthesis of 1,3-di(quinolin-5-yl)urea (DQ5U). Tri-ethylamine (0.2 mL) and 67.3 mg (0.226 mmol) of triphosgene were

added to a solution of 5-aminoquinoline (98.4 mg, 0.68 mmol) in 10 mL of dry dichloromethane; the resulting mixture was stirred at RT for 1 hour. The off-white precipitate formed was recovered through filtration and washed with dichloromethane (5 × 2 mL). Slow evaporation of a dimethyl sulfoxide solution yielded small block-shaped, colourless crystals. Yield: 20%.

^{1}H-NMR (DMSO-d_6, 400 MHz, ppm): 9.3 (2H, s), 8.945 (2H, m), 8.6 (2H, d, J = 8.8 Hz), 8.1 (2H, m), 7.7 (4H, m), 7.6 (2H, m). See Fig. ESI-3.†

Synthesis of 1-phenyl-3-(3,5-bis(pyrid-2-yl)-1,2,4-triazol-4-yl)-urea (PPT4U). A solution of phenyl isocyanate (0.27 mL, 2.5 mmol) in 8 mL of dichloromethane was added dropwise to a stirring solution of 4-amino-3,5-di-pyridyl-4*H*-1,2,4-triazole (0.6 g, 2.5 mmol) in 25 mL of dichloromethane over a period of 2 hours. The formed precipitate was collected through filtration and washed with dichloromethane, yielding 0.88 g of a white solid in the form of colourless needles (Form I). If Form I was left in the CH_2Cl_2 solution for 48 hours, plate-like crystals were obtained (Form II). The same behaviour was observed if the reaction was conducted in alcohols. Yield = 98%, m.p. = decomposes above 200 °C. 1H-NMR (400 MHz, DMSO-d_6, TMS) δ: 9.832 (s, 1H), 9.450 (s, 1H), 8.697–8.686 (d, 2H, CH), 8.118–8.098 (d, 2H), 8.034–7.991 (t, 2H), 7.544–7.551 (m, 2H). See Fig. ESI-4.† Form II could also be obtained directly *via* crystallization from acetone, or *via* kneading of Form I with a drop of methanol or ethanol.

Synthesis of $[Ag(PQ6U)_2]NO_3{\cdot}CH_3CN$. PQ6U (55 mg, 0.21 mmol) and $AgNO_3$ (17 mg, 0.104 mmol) were suspended in 6 mL of acetonitrile and heated up until a clear solution was obtained, which was allowed to slowly cool to room temperature. Colourless prisms suitable for X-ray diffraction grew overnight.

Synthesis of $[Ag(PQ6U)_2]NO_3$. PQ6U (0.061 mg, 0.23 mmol) and $AgNO_3$ (20 mg, 0.11 mmol) were suspended in *ca.* 7 mL of ether ethanol and heated up until a clear solution was obtained, which was allowed to slowly cool to room temperature. Colourless needle-shaped crystals of Form I suitable for X-ray diffraction grew overnight. Form I was also obtained upon desolvation of $[Ag(PQ6U)_2]NO_3{\cdot}CH_3CN$. When the synthesis was repeated after one month, only crystals of a second polymorph, Form II, were obtained (see below). Since then, we have not been able to reproduce Form I from any solvent: even if CH_3CN was used, only form II was directly obtained.

^{1}H-NMR spectroscopy

^{1}H-NMR spectra were recorded on a Varian Mercury400, chemical shifts of ^{1}H-NMR signals were expressed in parts per million (δ_H) using internal standard TMS (δ_H = 0.00). DMSO-d_6 was bought from the Cambridge Isotope Lab.

Structural characterization

Single-crystal data for all compounds (except PQ6U; see below) were collected using an Oxford X'Calibur S CCD diffractometer equipped with a graphite monochromator (Mo-Kα radiation, λ = 0.71073 Å) and operating at room temperature. Crystal data and details of measurement are listed in Tables 3 and 4. All non-hydrogen atoms were refined anisotropically; H_{NH} atoms were either directly located or added in calculated positions; H_{CH} atoms for all compounds were added in calculated positions and refined riding on their respective carbon atoms. SHELX97[13a] was used for structure solution and refinement on F^2; PLATON[13b] was used for hydrogen bonding analysis; Schakal99[13g] and Mercury[13e] were used for molecular graphics.

Table 3 Crystal data and details of measurements for the ligands

	PQ6U[a]	PiQ5U	DQ5U	PPT4U Form I (needle)	PPT4U Form II (plate)
Formula	$C_{16}H_{13}ON_3$	$C_{16}H_{13}ON_3$	$C_{18}H_{14}ON_2$	$C_{19}H_{15}N_6O$	$C_{19}H_{15}N_6O$
Fw (g mol^{-1})	263.29	263.29	314.34	343.37	343.37
a (Å)	19.5009(3)	24.020(2)	4.593(1)	11.128(1)	6.1197(4)
b (Å)	4.6309(7)	4.5893(3)	11.696(2)	10.2052(9)	8.0872(7)
c (Å)	14.8429(9)	11.828(1)	13.723(5)	16.432(2)	17.676(1)
α (°)	90	90	90	90	90
β (°)	99.0647(7)	96.411(7)	90	105.40(1)	91.449(6)
γ (°)	90	90	90	90	90
Z	4	4	2	4	2
V (Å^3)	1323.70(3)	1295.7(2)	737.2(6)	1799.0(3)	874.50(11)
D_{calc} (Mg m^{-3})	—	1.350	1.416	1.268	1.357
μ (mm^{-1})	—	0.087	0.092	0.084	0.091
Cryst. system	Monoclinic	Monoclinic	Orthorhombic	Monoclinic	Monoclinic
Space group	$P2_1/n$	$P2_1/c$	$P22_12_1$	$P2_1/c$	$P2_1$
Collected reflns	—	4414	2002	7850	4122
Indep. reflns	—	2641	1386	4037	2847
R_1 [on F_0^2, $I > 2\sigma(I)$]	—	0.0651	0.0503	0.0554	0.0560
wR_2 (all data)	—	0.01469	0.0760	0.1072	0.1258
R_{wp} (%)	9.44	—	—	—	
R_{exp} (%)	3.505	—	—	—	
χ^2	2.69	—	—		

[a] Structural solution from powder data.

Table 4 Crystal data and details of measurements for all complexes described

	$[Ag(PQ6U)_2]NO_3{\cdot}CH_3CN$	$[Ag(PQ6U)_2]NO_3$ Form I	$[Ag(PQ6U)_2]NO_3$ Form II	$[Ag(PQ5U)_2]NO_3$ Form V
Formula	$C_{34}H_{29}O_5N_8Ag$	$C_{32}H_{26}O_5N_7Ag$	$C_{32}H_{26}O_5N_7Ag$	$C_{32}H_{26}O_{10}N_7Ag$
Fw (g mol^{-1})	737.53	696.47	696.47	696.47
a (Å)	7.3672(2)	12.9856(7)	8.4802(6)	21.981(2)
b (Å)	9.0123(4)	16.975(1)	10.7958(10)	12.949(1)
c (Å)	25.5246(8)	27.061(1)	15.5706(9)	22.251(3)
α (°)	85.865(3)	90	86.193(6)	90
β (°)	87.607(3)	90	85.546(6)	101.16(1)
γ (°)	69.359(3)	90	87.377(7)	90
Z	2	8	2	8
V (Å^3)	1581.56(1)	5964.9(6)	1416.87(18)	6213.8(12)
D_{calc} (Mg m^{-3})	1.549	1.551	1.632	1.489
μ (mm^{-1})	0.694	0.730	0.768	0.701
Cryst. system	Triclinic	Orthorhombic	Triclinic	Monoclinic
Space group	$P\bar{1}$	*Pbca*	$P\bar{1}$	$P2_1/c$
Collected reflns	23 963	25 623	16 091	47 123
Indep. reflns	7541	7150	9317	12 967
R_1 [on F_0^2, $I > 2\sigma(I)$]	0.0966	0.0605	0.0702	0.1531
wR_2 (all data)	0.1728	0.1083	0.2429	0.4592

For phase identification purposes X-ray powder diffractograms in the 2θ range 5–40° (step size, 0.02°; time/step, 20 s; 0.04 rad soller; VxA 40 × 40) were collected on a Panalytical X'Pert PRO automated diffractometer equipped with an X'Celerator detector (Bragg–Brentano geometry), using CuKα radiation without a monochromator. The program Mercury[13e] was used for the calculation of X-ray powder patterns on the basis of single crystal data. In all cases the identity between bulk materials and single crystals was verified by comparing calculated and experimental powder diffraction patterns.

Structure determination and refinement of PQ6U from powder data

Powder diffraction data were analyzed with the software expo2010,[14a] which is designed to analyze monochromatic and non-monochromatic data. Peaks were automatically chosen in the 2θ range 5–40°, and a monoclinic cell was found (see Table 1), using the algorithm N-TREOR,[14b] with a volume of 1282.65 Å^3. The structure was then solved by simulated annealing using a molecular model built with the Avogadro software,[15] and refined by Rietveld analysis with the software TOPAS.[16]

A shifted Chebyshev function with 13 parameters and a Pseudo–Voigt function (TCHZ type) were used to fit background and peak shape, respectively. A spherical harmonics model was used to describe the preferred orientation. A rigid body was applied on the whole molecule. Bond distances and torsion angles of the urea group present in the PQ6U molecule were refined in a limited range around an equilibrium value. An overall thermal parameter for the C, N, O atoms of the PQ6U molecule was adopted. Refinement converged with χ^2 = 2.69, R_{wp} = 9.44%, R_{exp} = 3.505%. Fig. ESI-4† shows experimental, calculated and difference curves. Peaks at *ca.* 8° (101) and 18° (4 0 0) show a certain degree of preferred orientation that could not be modeled properly.

For structure solution and refinement purposes X-ray powder diffractograms in the 2θ range 5–60° (step size, 0.01°; time/step, 50 s; 0.02 rad soller; VxA 40 × 40) were collected on a Panalytical X'Pert PRO automated diffractometer equipped with an X'Celerator detector.

Thermogravimetric analysis (TGA)

TGA analyses were performed using a Perkin-Elmer TGA-7. Each sample, contained in a platinum crucible, was heated in a nitrogen flow (20 cm^3 min^{-1}) at a rate of 5 °C min^{-1}, up to decomposition. Sample weights were in the range 5–10 mg.

Photophysical measurements

Absorption spectra were recorded using a Perkin-Elmer Lambda 45 spectrophotometer. For the fluorescence spectroscopy measurements, uncorrected emission and corrected excitation spectra were obtained using a Perkin-Elmer LS 55 spectrofluorimeter. Luminescence quantum yields (uncertainty ± 15%) were determined using quinine sulfate in 0.05 M H_2SO_4 aqueous solution as a reference (Φ = 0.53). In order to allow comparison of emission intensities, corrections were performed for instrumental response, inner filter effects, and phototube sensitivity.[17] Values of log K_a were obtained by fitting spectrophotometric and spectrofluorimetric data with SPECFIT/32, a global analysis software. Mg^{2+}, Cu^{2+}, Ag^+, Hg^{2+} were delivered in the form of their trifluoromethanesulfonate salts dissolved in EtOH, while a $Cd(ClO_4)$ solution in EtOH was used as a source of Cd^{2+}. NO_3^-, F^-, Cl^-, Br^-, $H_2PO_4^-$ were delivered in the form of their tetrabutylammonium salts dissolved in EtOH, while a $CH_3COONa{\cdot}3H_2O$ solution in EtOH was used as a source of CH_3COO^- ions.

Photophysical measurements on gels were performed using an Edinburgh FLS920 equipped with photomultiplier Hamamatsu R928P and with Glann–Thompson polarizers for anisotropy measurements. The same instrument connected to a PCS900 PC card was used for the TCSPC experiments.

Fluorescence microscopy

Fluorescence imaging experiments were performed using an inverted microscope (Olympus IX71) equipped with an RGB camera (Basler ScA640-70GS), using as excitation light an Argon lamp with a 490 ± 18 nm excitation filter (MF390-18, Thorlabs).

The gel samples were spread between two glass slides in order to obtain a thin film which did not dry out during measurements.

Acknowledgements

We acknowledge financial support from the University of Bologna. The help of Dr Stefano Grilli with solution NMR measurements is acknowledged.

Notes and references

1 (*a*) R. G. Weiss and P. Terech, *Molecular Gels Materials with Self-Assembled Fibrillar Networks*, Springer, Dordrecht, 2006; (*b*) D. K. Smith, in *Organic Nanostructures*, ed. J. L. Atwood and J. W. Steed, WILEY-VCH, Weinheim, 2008, pp. 111–148; (*c*) J. W. Steed, *Chem. Commun.*, 2011, **47**, 1379–1383.

2 (*a*) N. M. Sangeetha and U. Maitra, *Chem. Soc. Rev.*, 2005, **34**, 821–836; (*b*) J. Raeburn, A. Zamith Cardoso and D. J. Adams, *Chem. Soc. Rev.*, 2013, **42**, 5143–5156; (*c*) P. Dastidar, *Chem. Soc. Rev.*, 2008, **37**, 2699–2715; (*d*) M.-O. M. Piepenbrock, G. O. Lloyd, N. Clarke and J. W. Steed, *Chem. Rev.*, 2010, **110**, 1960–2004.

3 (*a*) M.-O. M. Piepenbrock, N. Clarke and J. W. Steed, *Soft Matter*, 2011, **7**, 2412–2418; (*b*) J.-S. Shen, Y.-L. Chen, J.-L. Huang, J.-D. Chen, C. Zhao, Y.-Q. Zheng, T. Yu, Y. Yanga and H.-W. Zhang, *Soft Matter*, 2013, **9**, 2017–2023.

4 J. A. Foster, M.-O. M. Piepenbrock, G. O. Lloyd, N. Clarke, J. A. K. Howard and J. W. Steed, *Nat. Chem.*, 2010, **2**, 1037–1043.

5 (*a*) Y. J. Seo, S. Bhuniya and B. H. Kim, *Chem. Commun.*, 2007, 1804–1806; (*b*) S. Debnath, A. Shome, D. Das and P. K. Das, *J. Phys. Chem. B*, 2010, **114**, 4407–4415; (*c*) S. Sutton, N. L. Campbell, A. I. Cooper, M. Kirkland, W. J. Frith and D. J. Adams, *Langmuir*, 2009, **25**, 10285–10291; (*d*) J. A. Saez, B. Escuder and J. F. Miravet, *Tetrahedron*, 2010, **66**, 2614–2618.

6 (*a*) A. R. Hirst, B. Escuder, J. F. Miravet and D. K. Smith, *Angew. Chem., Int. Ed.*, 2008, **47**, 8002–8018; (*b*) N. M. Sangeetha and U. Maitra, *Chem. Soc. Rev.*, 2005, **34**, 821–836; (*c*) L. A. Estroff and A. D. Hamilton, *Chem. Rev.*, 2004, **104**, 1201–1217.

7 (*a*) G. Bühler, M. C. Feiters, R. J. M. Nolte and K. H. DöItz, *Angew. Chem., Int. Ed.*, 2003, **115**, 2599–2602; (*b*) G. Bühler, M. C. Feiters, R. J. M. Nolte and K. H. DöItz, *Angew. Chem., Int. Ed.*, 2003, **42**, 2494–2497.

8 (*a*) J. A. Foster, M.-O. M. Piepenbrock, G. O. Lloyd, N. Clarke, J. A. K. Howard and J. W. Steed, *Nat. Chem.*, 2010, **2**, 1037–1043; (*b*) A. Yiu-Yan Tam and V. Wing-Wah Yam, *Chem. Soc. Rev.*, 2013, **42**, 1540–1567; (*c*) K. A. Houton, K. L. Morris, L. Chen, M. Schmidtmann, J. T. A. Jones, L. C. Serpell, G. O. Lloyd and D. J. Adams, *Langmuir*, 2012, **28**, 9797–9806; (*d*) U. K. Das, V. G. Puranik and P. Dastidar, *Cryst. Growth Des.*, 2012, **12**, 5864–5868; (*e*) U. K. Das and P. Dastidar, *Chem.–Eur. J.*, 2012, **18**, 13079–13090; (*f*) L. Meazza, J. A. Foster, K. Fucke, P. Metrangolo, G. Resnati and J. W. Steed, *Nat. Chem.*, 2013, **5**, 42–47.

9 D. Braga, S. d'Agostino, E. D'Amen and F. Grepioni, *Chem. Commun.*, 2011, **47**, 5154–5156.

10 D. Kalita, R. Sarma and J. B. Baruah, *CrystEngComm*, 2009, **11**, 803–810.

11 (*a*) J. Bernstein, R. E. Davis, L. Shimoni and N.-L. Chang, *Angew. Chem., Int. Ed. Engl.*, 1995, **34**, 1555–1573; (*b*) M. C. Etter, *Acc. Chem. Res.*, 1990, **23**, 120; (*c*) M. C. Etter, J. C. MacDonald and J. Bernstein, *Acta Crystallogr., Sect. B: Struct. Sci.*, 1990, **46**, 256–262.

12 (*a*) W. R. Moomaw and M. F. Anton, *J. Phys. Chem.*, 1976, **80**, 2243–2247; (*b*) F. R. Stermitz, C. C. Wei and C. M. O'Donnell, *J. Am. Chem. Soc.*, 1970, **92**, 2745–2752.

13 (*a*) G. M. Sheldrick, *SHELX97, Program for Crystal Structure Determination*, University of Göttingen, Göttingen, Germany, 1997; (*b*) A. L. Speck, PLATON, *Acta Crystallogr., Sect. A: Fundam. Crystallogr.*, 1990, **46**, C34; (*c*) C. F. Macrae, I. J. Bruno, J. A. Chisholm, P. R. Edgington, P. McCabe, E. Pidcock, L. Rodriguez-Monge, R. Taylor, J. van de Streek and P. A. J. Wood, *Appl. Crystallogr.*, 2008, **41**, 466–470; (*d*) G. M. Sheldrick, *SHELX97, Program for Crystal Structure Determination*, University of Göttingen, Göttingen, Germany, 1997; (*e*) M. C. Burla, R. Caliandro, M. Camalli, B. Carrozzini, G. L. Cascarano, L. De Caro, C. Giacovazzo, G. Polidori, D. Siliqi and R. Spagna, *J. Appl. Crystallogr.*, 2007, **40**, 609–613; (*f*) A. L. Speck, PLATON, *Acta Crystallogr., Sect. A: Fundam. Crystallogr.*, 1990, **46**, C34; (*g*) E. Keller, *SCHAKAL99, Graphical Representation of Molecular Models*, University of Freiburg, Freiburg, Germany, 1999.

14 (*a*) A. Altomare, M. Camalli, C. Cuocci and R. Rizzi, *J. Appl. Crystallogr.*, 2009, **42**, 1197–1202; (*b*) A. Altomare, C. Giacovazzo, A. Molinterni and R. Rizzi, *J. Appl. Crystallogr.*, 2001, **34**, 704–709.

15 Avogadro: an open-source molecular builder and visualization tool. M. D. Hanwell, D. E. Curtis, D. C. Lonie, T. Vandermeersch, E. Zurek and G. R. Hutchison, *J. Cheminf*, 2012, 4–17.

16 A. Cohelo, *TOPAS-Academic*, Coelho Software, Brisbane, Australia, 2007.

17 A. Credi and L. Prodi, *Spectrochim. Acta, Part A*, 1998, **54**, 159–170.

